Supplementary Information (SI) for Soft Matter.
This journal is © The Royal Society of Chemistry 2026

Supplementary Information

Nudging Cell Migration from Within through Microrod-Induced Morphological Deformation

Masayuki Hayakawa[*a], Tatsuya Tanaka[b], and Hiroaki Suzuki[b]

[a.] Department of Mechanical Engineering, Kyoto Institute of Technology, Goshokaido-cho, Matsugasaki, Sakyo-ku, Kyoto, 606-8585, Japan.

Email: hayakawa@kit.ac.jp

[b.] Graduate School of Science and Engineering, Chuo University, Kasuga 1-13-27, Bunkyo-ku, Tokyo, 112-8551, Japan.

Movie Captions

Movie S1. A typical KI cell showing no interaction with a glass microrod.
The cell did not adhere to or internalize the microrod. The movie (total duration = 300 s) is shown at approximately 100× real time.

Movie S2. Partial attachment between a KI cell and a glass microrod.
One end of the microrod adhered to the cell surface without being fully engulfed. The movie (total duration = 300 s) is shown at approximately 100× real time.

Movie S3. Internalization of a glass microrod by a KI cell.
The microrod was completely engulfed and internalized within the cell. The movie (total duration = 300 s) is shown at approximately 100× real time.

Movie S4. Migration of cell–rod composites.
Elongated morphological dynamics of a cell–rod composite. Left: microscopic observation; right: corresponding cell contour. The movie (total duration = 120 s) is shown at approximately 40× real time.

Movie S5. Migration of cell–rod composites.
Cells indicated by magenta arrows represent cell–rod composites. The movie (total duration = 1800 s) is shown at approximately 410× real time.

Movie S6. Another example of the migration of cell–rod composites.
Cells indicated by magenta arrows represent cell–rod composites. The movie (total duration = 1800 s) is shown at approximately 410× real time.

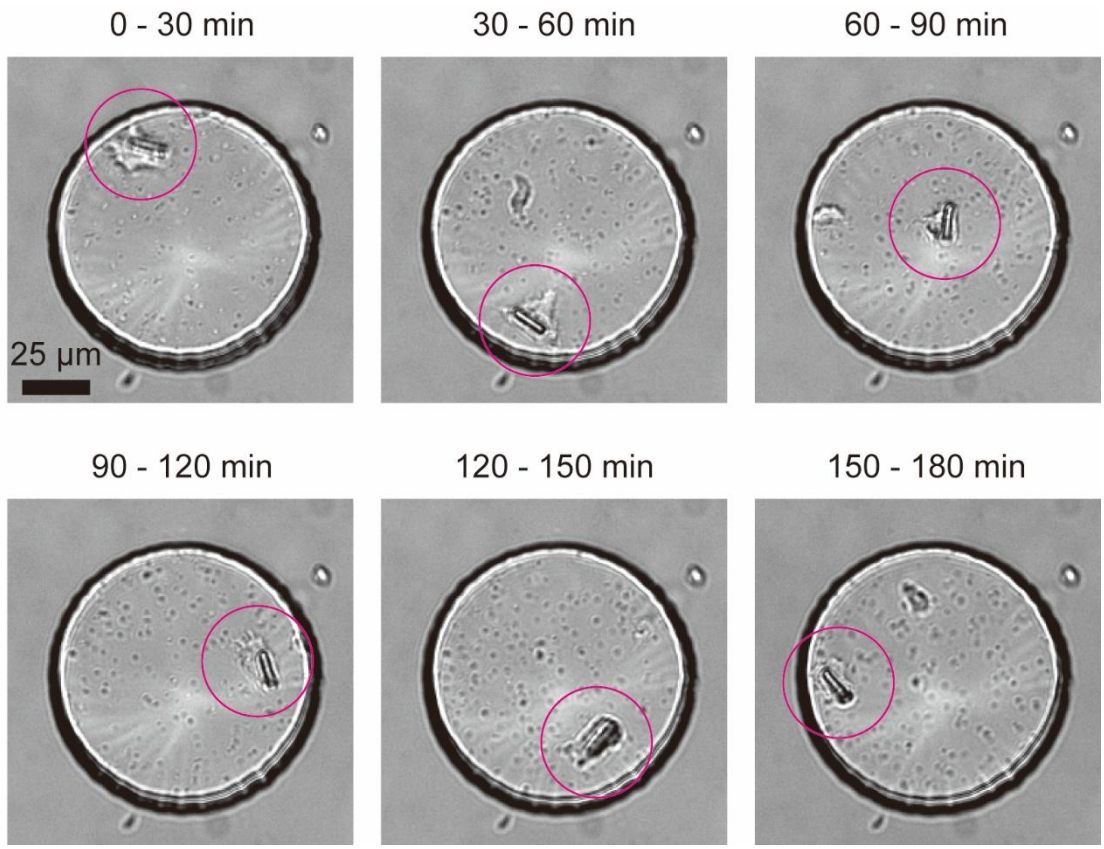

Figure S1. Representative snapshots of a cell–rod composite migrating in a PDMS chamber over 3 h.
Bright-field images of a representative cell–rod composite in a PDMS chamber. Each snapshot was selected as a representative frame from the indicated 30 min time window: 0–30, 30–60, 60–90, 90–120, 120–150, and 150–180 min. Magenta circles indicate the cell–rod composite. A mixture of KI cells and microrods was loaded into the PDMS chamber overnight before imaging. The chamber consisted of a cylindrical PDMS microwell (diameter 100 µm, height 30 µm) and sealed with mineral oil to prevent evaporation. In this experiment, the microrod remained fully internalized and no rod ejection was observed during the observation period.

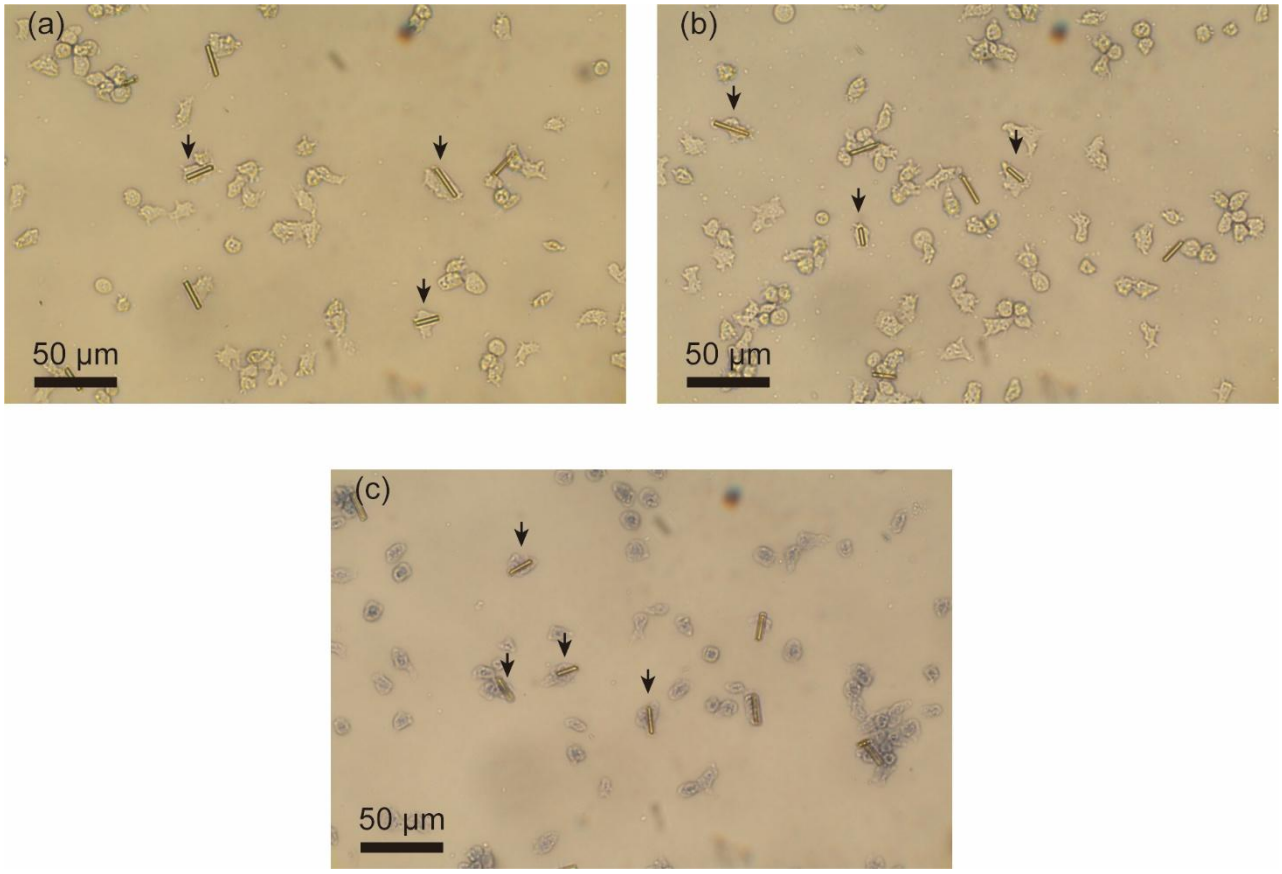

Figure S2. Trypan blue exclusion assay on substrate-adhered KI cells and cell–rod composites.

(a, b) Representative bright-field images after trypan blue staining showing KI cells without microrods and cell–rod composites (indicated by black arrows), both of which largely excluded trypan blue after overnight incubation. (c) Positive control: the same staining procedure applied after ethanol pretreatment (70% ethanol, 3 min) resulted in dye uptake, confirming assay functionality.

Assay protocol: KI cells were mixed with microrods in phosphate buffer (PB) and deposited on a 22 mm × 22 mm coverslip. Samples were incubated overnight under the same conditions as the internalization experiments. The supernatant PB was gently removed, the coverslip was immersed in 0.2% trypan blue in PB for 3 min, briefly rinsed once in PB, transferred to fresh PB, and immediately imaged.

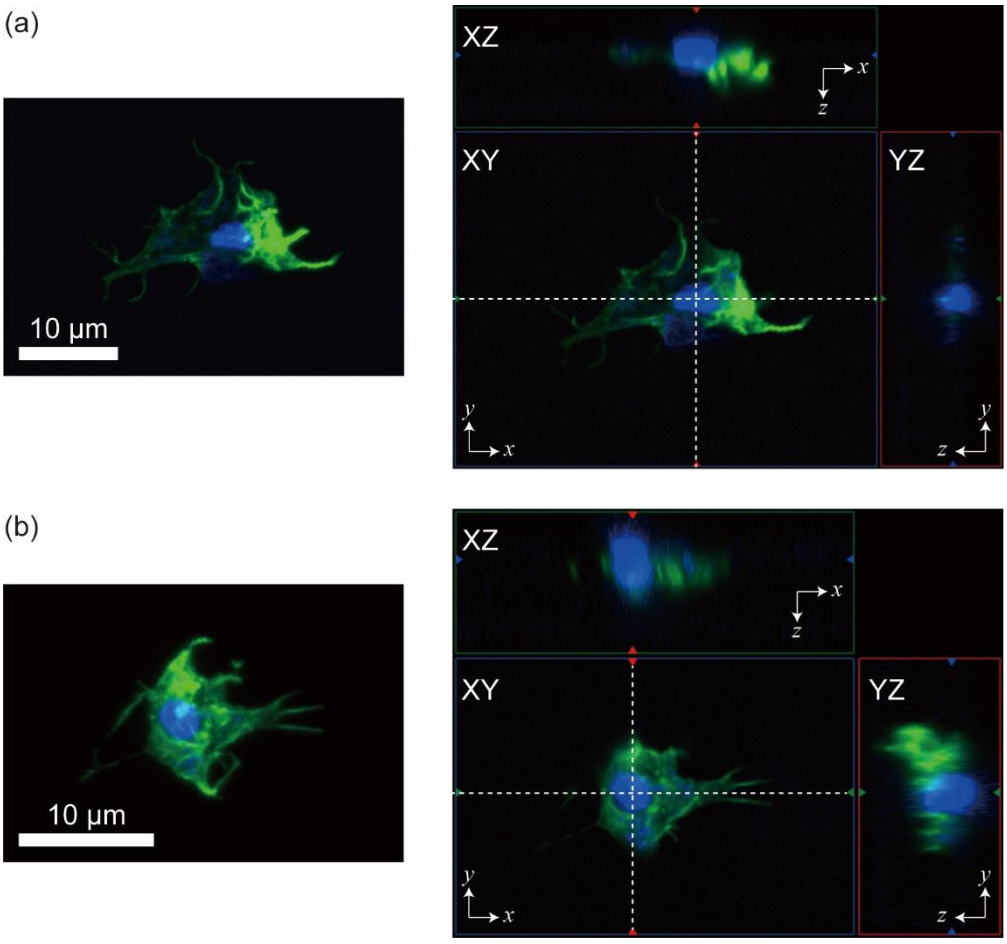

Figure S3. Confocal microscopy images of fixed cells stained with phalloidin (green) and Hoechst (blue)

(a, b) Left panels: Maximum intensity projection images of representative cells. Right panels: Orthogonal views corresponding to the cells shown in the left panels.

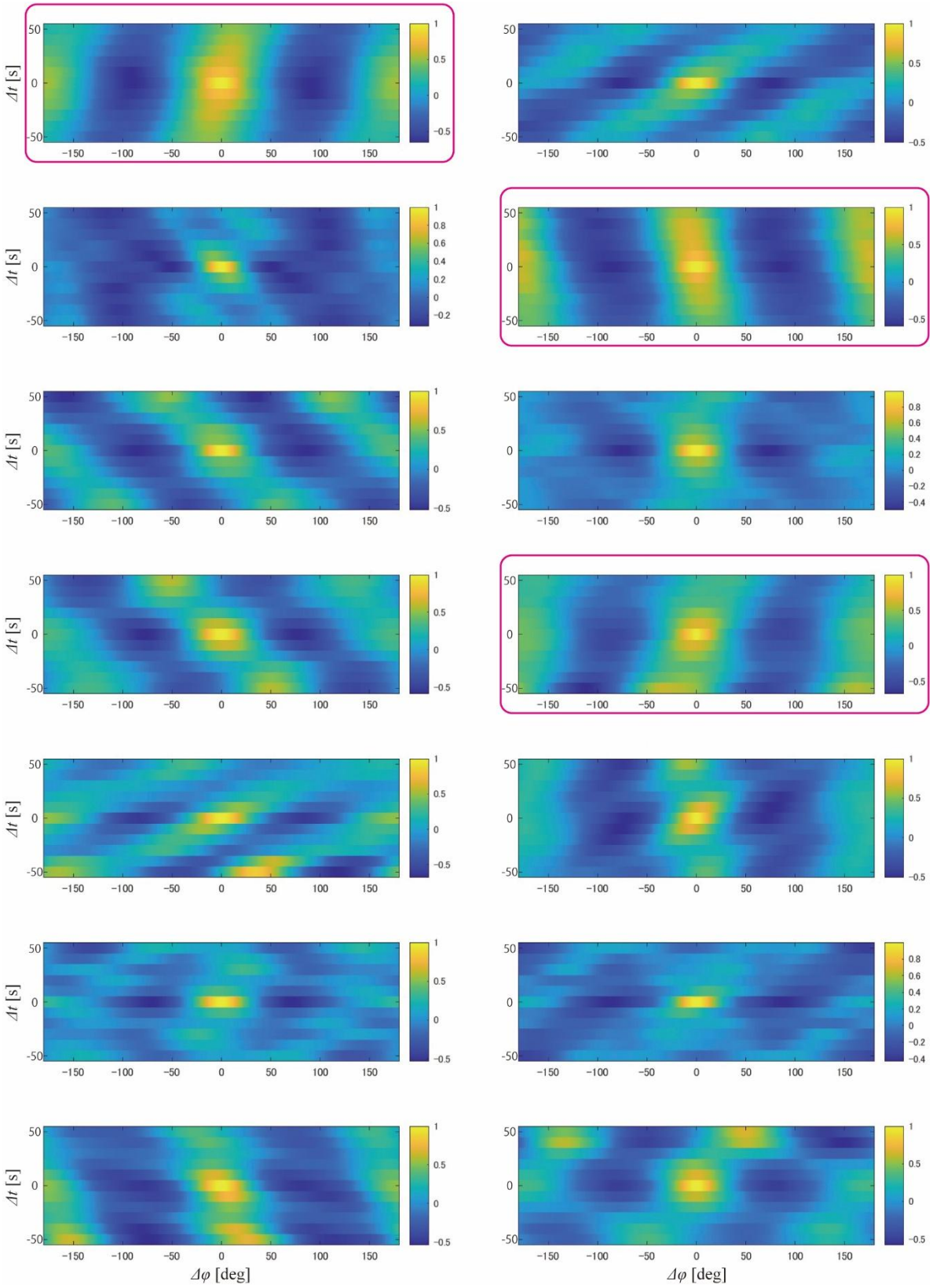

Figure S4. Spatiotemporal dynamics of cell morphology (Control cells)

Mapping of $C_{Amp}(\Delta\phi, \Delta t)$. Patterns surrounded by magenta rounded rectangles indicate elongation pattern.

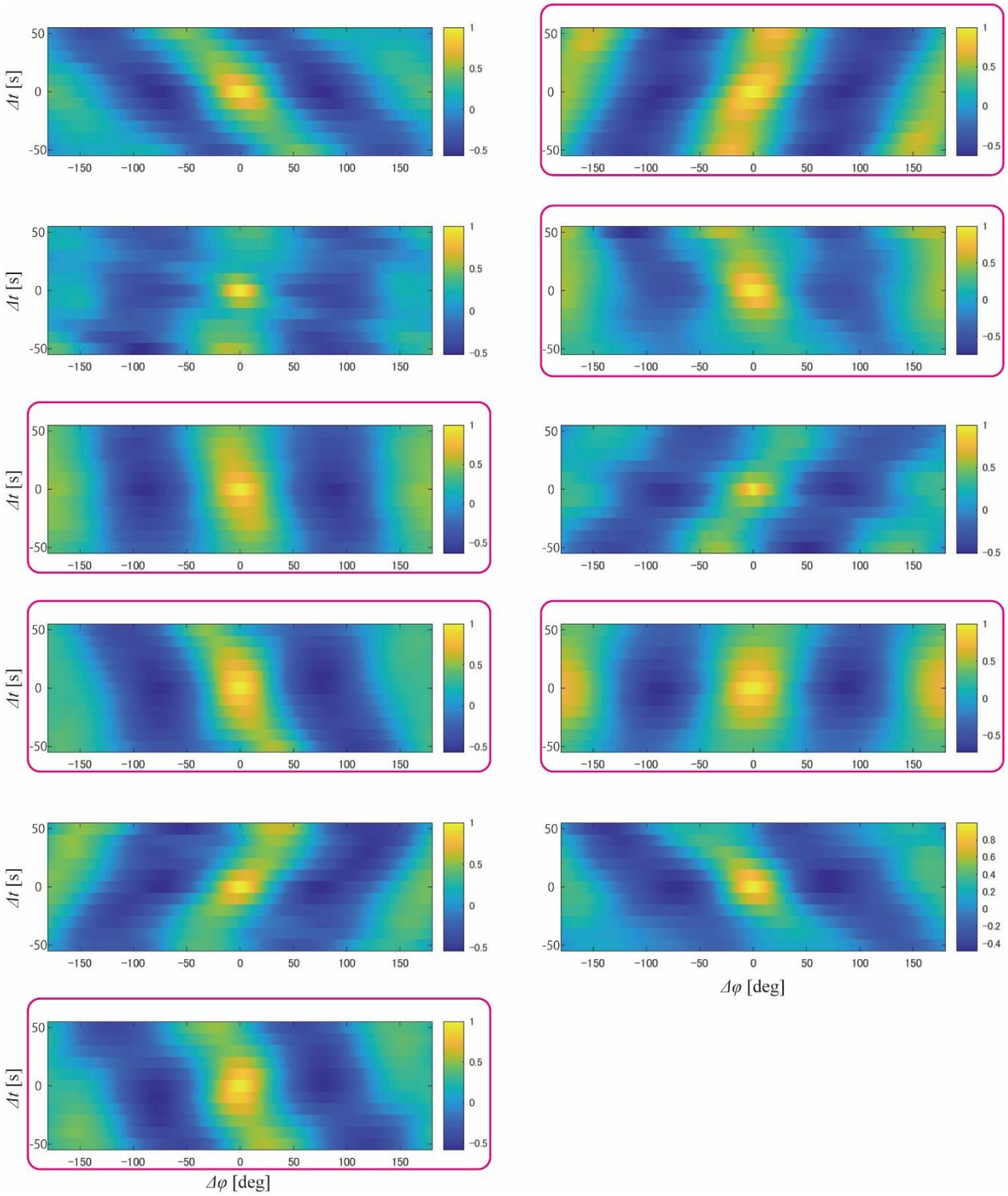

Figure S5. Spatiotemporal dynamics of cell morphology (Cell–rod composites)

Mapping of $C_{Amp}(\Delta\phi, \Delta t)$. Patterns surrounded by magenta rounded rectangles indicate elongation pattern.

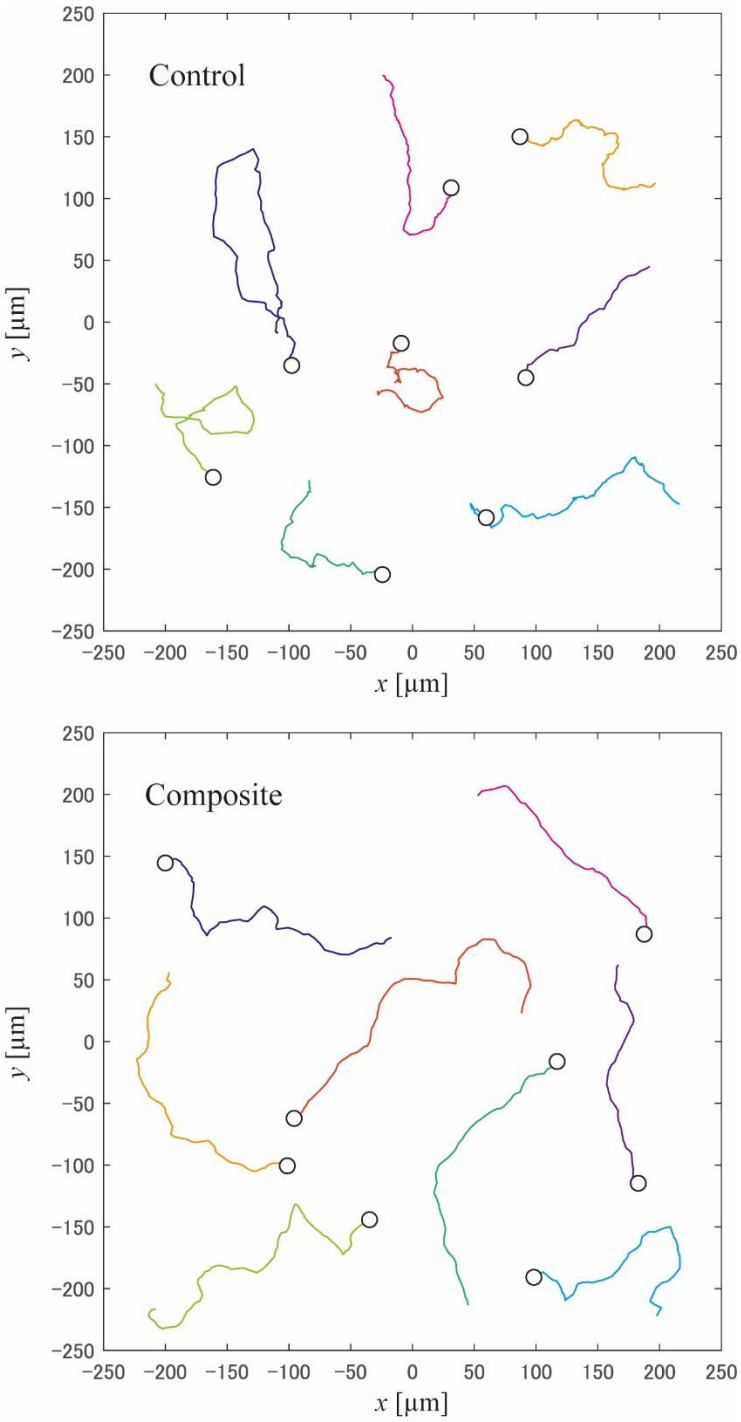

Figure S6. Typical trajectories of migrating cells (top: controls; bottom: cell–rod composites)

Circles indicate the starting points of tracking, and tracking durations ranged from 480 s to 1800 s.

Table S1. Parameters from persistent random-walk fits to the MSD.

Values are shown as median [95% CI].

	v (μm/s)	τ (s)	L_p (μm)
Control	0.185 [0.125, 0.267]	83.7 [40, 258]	15.6 [8.93, 33.6]
Cell–rod composites	0.181 [0.156, 0.220]	562 [233, 1000]	102 [50.3, 177]

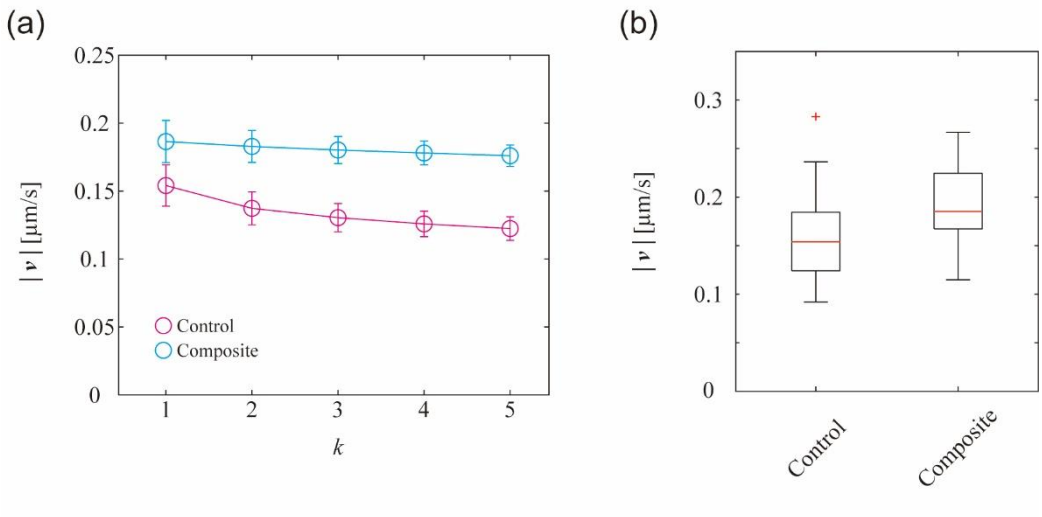

Figure S7. Dependence of the measured apparent migration speed on the discretization window *k*.

The apparent speed was calculated from cell trajectories as

$$|v| = \frac{|\boldsymbol{r}(t + k\Delta t) - \boldsymbol{r}(t)|}{k\Delta t},$$

with imaging interval $\Delta t = 20$ s. (a) $|v|$ for cell–rod composite (cyan circle) and control (magenta circle) as a function of k. Error bars indicate SE across cells (Control: $\mathrm{N} = 32$, Composite: $\mathrm{N} = 30$). (b) Comparison of mean apparent migration speeds $|v|$ at $k = 1$.